International Journal of Climatology

RMetS Royal Meteorological Society

High-resolution monthly precipitation climatologies over Norway (1981–2010): joining numerical model datasets and in-situ observations

Journal:	*International Journal of Climatology*
Manuscript ID	JOC-18-0496.R1
Wiley - Manuscript type:	Research Article
Date Submitted by the Author:	n/a
Complete List of Authors:	Crespi, Alice; Università degli Studi di Milano, Department of Environmental Science and Policy Lussana, Cristian; Norwegian Meteorological Institute, Observation and Climate BRUNETTI, Michele; National Research Council, Institute of Atmospheric Sciences and Climate Dobler, Andreas; Norwegian Meterological Institute, Observation and Climate Maugeri, Maurizio; Università degli Studi di Milano, Department of Environmental Science and Policy; National Research Council, Institute of Atmospheric Sciences and Climate Tveito, Ole; Norwegian Meteorological Institute, Observation and Climate
Keywords:	Norway, precipitation, interpolation model, HCLIM-AROME, rain-gauges
Country Keywords:	Italy, Norway

High-resolution monthly precipitation climatologies over Norway (1981–2010): joining numerical model datasets and in-situ observations

Alice Crespi*, Cristian Lussana, Michele Brunetti, Andreas Dobler, Maurizio Maugeri, Ole Einar Tveito

The paper presents the 1981–2010 monthly precipitation climatologies over Norway at 1 km grid spacing. The climatologies are computed by an interpolation scheme (HCLIM+RK) combining the in-situ observations with the regional climate model dataset HCLIM-AROME, based on the dynamical downscaling of the global ERA-Interim reanalysis. The comparison with methods using observations only proved that HCLIM+RK improves the accuracy of Norwegian climatologies and provides reliable precipitation patterns also over the remote areas not covered by rain-gauges.

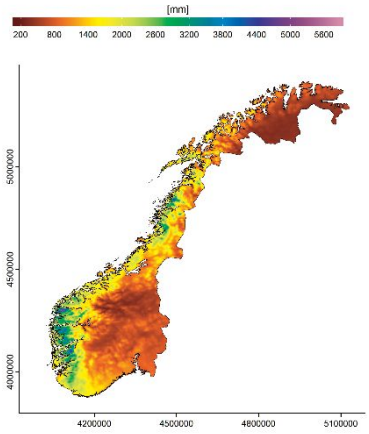

High-resolution monthly precipitation climatologies over Norway (1981–2010): joining numerical model datasets and in-situ observations

Alice Crespi[1], Cristian Lussana[2], Michele Brunetti[3], Andreas Dobler[2], Maurizio Maugeri[1,3], Ole Einar Tveito[2]

[1]*Department of Environmental Science and Policy, Università degli Studi di Milano, Milan, 20133, Italy*

[2]*The Norwegian Meteorological Institute, Oslo, 0313, Norway*

[3]*Institute of Atmospheric Sciences and Climate, ISAC-CNR, Bologna, 40129, Italy*

Corresponding author: Alice Crespi, email: alice.crespi@unimi.it, phone: +39 3477777563

Running head: Norwegian monthly precipitation climatologies

Keywords: Norway, precipitation, interpolation model, HCLIM-AROME, rain-gauges

Abstract

The 1981–2010 monthly precipitation climatologies for Norway at 1 km resolution are presented. They are computed by an interpolation procedure (HCLIM+RK) combining the output from a numerical model with the in-situ observations. Specifically, the regional climate model dataset HCLIM-AROME, based on the dynamical downscaling of the global ERA-Interim reanalysis onto 2.5 km resolution, is considered together with 2009 rain-gauges located within the model domain. The precipitation climatologies are defined by superimposing the grid of 1981–2010 monthly normals from the numerical model and the kriging interpolation of station residuals. The combined approach aims at improving the quality of gridded climatologies and at providing reliable precipitation gradients also over those remote Norwegian regions not covered by observations, especially over the northernmost mountainous areas. The integration of rain-gauge data greatly reduces the original HCLIM-AROME biases. The HCLIM+RK errors obtained from the leave-one-out station validation turn out to be lower than those provided by two considered interpolation schemes based on observations only: a multi-linear local regression kriging (MLRK) and a local weighted linear regression (LWLR). As average over all months, the mean absolute (percentage) error is 10.0 mm

(11%) for HCLIM+RK, and 11.4 (12%) and 11.6 mm (12%) for MLRK and LWLR, respectively. In addition, by comparing the results at both station and grid cell level, the accuracy of MLRK and LWLR is more sensitive to the spatial variability of station distribution over the domain and their interpolated fields are more affected by discontinuities and outliers, especially over those areas not covered by the rain-gauge network. The obtained HCLIM+RK climatologies clearly depict the main West-to-East gradient occurring from the orographic precipitation regime of the coast to the more continental climate of the inland and it allows to point out the features of the climatic subzones of Norway.

1. Introduction

Gridded climatological datasets of surface precipitation represent valuable information sources for both researchers and decision makers in a wide range of fields, such as energy production, management and conservation of natural resources and agriculture (Prein and Gobiet, 2017). The availability of accurate high-resolution descriptions of spatial distribution of the precipitation normals over the territory is particularly relevant for those countries, such as Norway, whose electricity sector relies primarily on hydropower (Dyrrdal et al., 2015).

The reconstruction of conventional climatological datasets, as defined by Simmons et al. (2017), requires both dense rain-gauge networks and statistical interpolation approaches able to capture the interactions between atmospheric circulation and the surface (Henn et al., 2018). In fact, precipitation distribution is found to be strongly influenced by the main geographical features, such as elevation, sea nearness and slope conditions, and these relationships could highly vary at local level (Daly et al, 2008). A wide selection of statistical schemes has been developed and applied so far to project monthly precipitation normals from station sites onto the unsampled points of high-resolution grids, such as geostatistical approaches based on kriging and all its variants (Goovaerts, 2000; Hengl, 2009), regression-based models (Daly, 2002; Crespi et al., 2018), spline and inverse distance weighting interpolation (Boer et al., 2001). The uneven spatial coverage of observational data could significantly

affect the interpolation accuracy especially in highly variable terrains where the model predictions could be derived from rain-gauges located at distant and very different environments.

The Norwegian Meteorological Institute (MET) provided two versions of the *seNorge* gridded dataset for daily precipitation over Norway at 1 km resolution: one is based on a triangulation procedure with altitude corrections (Tveito et al., 2005; Mohr, 2008; 2009) and the other is based on a multi-scale optimal interpolation approach (Lussana et al., 2018). The distribution of Norwegian station network is very sparse over the northern inland and the scarcely sampled high-elevation areas significantly limit the ability of observation-based models to capture the actual conditions occurring over these regions. In particular, remarkable underestimations in gridded precipitation values are found to occur over the mountainous inland where the complex environment prevents the management of manual stations and limits the availability of dense observations (Lussana et al., 2018). Only in recent years, some new automatic rain-gauges have been established in these areas and their data have improved the monitoring applications even though the short length of the new records is not yet suitable for climatological studies.

In this study, we aim to combine two data sources, such as in-situ observations and numerical model outputs in order to obtain as accurate as possible monthly precipitation climatologies even in data-sparse areas over complex terrains. The advancements in the accuracy and spatial resolution of numerical models in fact provided new data and information in the last years, which started to be used in the inter-comparisons with observation-based gridded datasets (Haylock et al., 2008; Dyrrdal et al., 2018) as well as in climatological studies (Karger et al., 2017; Berthou et al., 2018). In particular, regional model reanalyses are primarily relevant for climatological applications because of the high spatial resolution (almost comparable to operational numerical weather prediction systems, NWP) of their long-term gridded datasets (Isotta et al., 2015; Jermey and Renshaw, 2016). The high-resolution of the regional reanalysis datasets is found to improve the description of precipitation fields in comparison with the global ones, especially for extreme events, even though reanalyses are affected by significant biases, shifts in regional anomalies and inaccuracies in mountain-valley contrasts.

MET has recently produced a climate model dataset of precipitation covering the Norwegian mainland at 2.5 km resolution over the period July 2003 to December 2016. The dataset is based on the dynamical downscaling of the global ERA-Interim reanalysis (Dee et al., 2011) using HCLIM-AROME, the climate model version of the HARMONIE (HIRLAM ALADIN Research towards Mesoscale Operational NWP In Europe) NWP model framework (Lind et al., 2016). The model includes a set of different physics packages adapted for different horizontal resolutions. The high spatial resolution of the HCLIM-AROME model is suitable to provide useful information over the remote regions not covered by in-situ observations. The overall model setup is similar to the operational AROME-MetCoOp model, which provides realistic precipitation patterns especially where orographically forced precipitation is the dominant mechanism (Müller et al., 2017).

In this framework, we developed and applied an interpolation approach in which rain-gauge observations and the numerical model output are used together to provide the 1981–2010 monthly precipitation climatologies over Norway at 1 km grid spacing. In this scheme, hereafter referred to as HCLIM+RK, the grids of monthly precipitation normals derived from HCLIM-AROME dataset are considered as background and a kriging interpolation procedure is applied to adjust the original fields by means of station residuals, i.e. the differences between the station normals and the numerical model estimates at the closest grid cells. This procedure allows both to exploit the spatial precipitation gradients resolved by HCLIM-AROME, especially over the regions not covered by stations, and to improve the accuracy of resulting climatologies by integrating the available in-situ observations to correct the numerical model biases. In order to compute the 30-year climatologies, the HCLIM-AROME dataset was extended back to 1981 using available station records and a reconstruction procedure based on multiplicative anomalies.

In the present work the features of HCLIM+RK method are extensively investigated and discussed and the computed 1981–2010 monthly precipitation climatologies over Norway are presented. Moreover, in order to assess the improvements provided to Norwegian climatologies by the combination of numerical model datasets and rain-gauge data, HCLIM+RK performances are

compared to those obtained by two statistical methods based on observations only: a multi-linear local regression kriging (MLRK) and a local weighted linear regression (LWLR) of precipitation *versus* elevation, based on ideas from PRISM (Daly, 2002).

2. Data

2.1 Precipitation data from the rain-gauge network

The observational database considered to reconstruct the 1981–2010 monthly precipitation climatologies over Norway is composed by more than 2000 station records of monthly precipitation covering the HCLIM-AROME domain (Figure 1). The Norwegian station series were retrieved from the MET Norway Climate daily database (KDVH) and they were integrated with the daily records contained in the European Climate Assessment and Dataset (ECA&D) for the surrounding countries. The monthly database was checked for quality in order to detect and correct spurious entries, duplicates and erroneous locations. In particular, following the procedure described in Crespi et al. (2018), each measured series was compared to the simulated one by means of neighbouring station data and reconstruction errors were computed in terms of Mean Absolute Error (MAE) and Root Mean Square Error (RMSE). High errors allowed to point out and remove single problematic periods in a record or to discard stations for which the observed values completely mismatched the simulated ones.

After removing gross data errors in both monthly and daily series, the gap-filling procedure described in Golzio et al. (2018) was applied to daily records in order to maximize the number and length of monthly data series available for climatological purposes. Monthly precipitation series were computed again for each station from filled daily records and whenever daily data were still missing, the corresponding monthly total was not computed. On average, the filling procedure allowed to reconstruct 3% of daily gaps which led to increase the available monthly precipitation totals for each station of about 12%. Stations with fewer than 10 years of available data, also after the gap-filling, were definitely discarded from the database. After these procedures, the 1981–2010 monthly precipitation normals were computed for each series and, whenever this period was partially or

completely unavailable, missing months were reconstructed by a procedure based on multiplicative anomalies of neighbouring stations (Crespi et al., 2018). Since a large fraction of stations (52%) had more than 30% of missing data in the reference period, this procedure allowed to prevent monthly normals from being biased by a lower fraction of monthly data entering in the average computation. Finally, the 1981–2010 precipitation normals were available for 2009 sites, 1043 out of them located in Norway. However, Norwegian sites are unevenly distributed over the country: data coverage is generally higher in the South (below 63°18'N) with about one station per 250 km^2 and it decreases significantly towards the North (above 63°18'N) with about one station per 500 km^2 (Figure 1). Moreover, most rain-gauges are located at low-elevation and only 15% and 1% of stations are above 500 and 1000 m a.s.l., respectively, so that the grid cells at higher elevation (47% and 15% of the total are above 500 and 1000 m a.s.l., respectively) are mostly or completely uncovered by in-situ observations (Figure 2).

2.2 HCLIM-AROME numerical model dataset of monthly precipitation

The HCLIM-AROME dataset of monthly precipitation over Norway was retrieved from the hourly precipitation fields at 2.5 km grid spacing computed by the climate model version of HARMONIE (version cy38h1.2). To perform the high-resolution convection permitting simulations, the model was set up with the AROME physics (Seity et al., 2011) and the SURFEX surface scheme (Masson et al., 2013). The model was run from July 2003 to December 2016 and it covers the whole Norwegian mainland and parts of Sweden, Finland and Russia.

The series of monthly totals were computed for each grid cell by summing the hourly precipitation and the data were downscaled onto the target 1 km grid, which is based on the two-dimensional Lambert Azimuthal Equal Area coordinate reference system INSPIRE: ETRS89-LAEA proposed as the multipurpose Pan-European standard from the European Commission (https://inspire.ec.europa.eu/id/document/tg/gg).

In order to obtain the 1981–2010 mean monthly HCLIM-AROME fields, the 2003–2016 monthly precipitation series of all cells in the 2.5 km grid were extended back to January 1981 by means of

available in-situ observations. For this purpose, the same reconstruction method applied to fill monthly station gaps and based on multiplicative anomalies was considered. More precisely, each missing monthly value of all the HCLIM-AROME grid points ($p_m^{HCLIM-AROME}$) was reconstructed by selecting the 5 closest stations with at least 9 years of common data in the period 2003–2016 and a valid entry for the month under reconstruction. From the selected station data, 5 simulated values for month m at the target cell were computed by rescaling each rain-gauge entry $p_{m,i}$ by the ratio between the monthly means of HCLIM-AROME cell values ($\overline{p_{m,i}^{HCLIM-AROME}}$) and station observations ($\overline{p_{m,i}}$) over the available years in the period 2003–2016:

$$p_{m,i}^{HCLIM-AROME} = p_{m,i} \cdot \frac{\overline{p_{m,i}^{HCLIM-AROME}}}{\overline{p_{m,i}}} \quad (i = 1, \ldots, 5) \qquad (1)$$

The final estimate is defined as the weighted mean of the 5 simulations where the station weight is expressed as a Gaussian function of the radial distance from the considered cell (Crespi et al., 2018). After the reconstruction, the 1981–2010 HCLIM-AROME monthly normals were computed and downscaled to the target 1 km resolution grid by means of a bilinear interpolation procedure.

3. Methods

3.1 The combined interpolation scheme: HCLIM+RK

In HCLIM+RK scheme the residuals between each 1981–2010 station normal and the corresponding value at the closest cell of HCLIM-AROME grid rescaled at 1 km resolution are computed for each month and their spatial distribution is modelled by the kriging procedure. The sample variogram is reconstructed from all the station pairs within 300 km and by setting the bin width to 15 km, while the fitted variogram is obtained by considering the exponential model.

The final value of the 1981–2010 precipitation normal for the month *m* at cell (x,y) is obtained by adding the interpolated station residuals to the corresponding monthly normal from the downscaled HCLIM-AROME background:

$$p_m(x,y) = p_m^{HCLIM-AROME}(x,y) + \mathbf{k}^{\mathbf{T}}(x,y) \cdot \boldsymbol{\varepsilon} \qquad (2)$$

where $\mathbf{k}\,(x,y)$ is the vector of kriging weights at the cell (x,y) and $\boldsymbol{\varepsilon}$ are the station residuals.

3.2 Observation-based interpolation methods

In MLRK the precipitation normal for month m at each grid cell (x,y) is computed by applying the residual regression kriging with the regression based on a local multi-linear relationship between precipitation and several geographical predictors:

$$p_m(x,y) = \sum_{j=1}^{N} \alpha_{j,m}(x,y) \cdot q_{j,m}(x,y) + \mathbf{k}^{\mathbf{T}}(x,y) \cdot \boldsymbol{\varepsilon} \quad (3)$$

where N is the numbers of geographical predictors, $\boldsymbol{\alpha}$ and $\boldsymbol{q}$ are the vectors of regression coefficients and predictor values at target site (x,y), respectively, $\mathbf{k}$ (x,y) is the vector of kriging weights and $\boldsymbol{\varepsilon}$ are the residuals between observed normals and regression estimates at station locations. Latitude, longitude, elevation and sea distance are chosen as regression geographical predictors for all months while $\boldsymbol{\alpha}$ are monthly estimated for each grid cell by the least-square method considering precipitation normals and geographical features of all sample sites within 100 km from the point. If fewer than 100 stations are available for regression within this distance, searching radius is incremented by 10 km steps until the minimum threshold is reached. Both the searching radius and the number of stations entering in the regression are defined by the minimization of model errors (see below for details on model errors). Also in this case, the experimental variogram is defined by considering a bin width of 15 km and all the station pairs within 300 km and it is fitted by the exponential model.

In LWLR the monthly precipitation normals at each grid cell (x,y) are modelled by using elevation as the main geographical predictor:

$$p_m(x,y) = a_m(x,y) + b_m(x,y) \cdot h(x,y) \quad (4)$$

where $h(x,y)$ is the elevation of cell (x,y) and $a_m(x,y)$ and $b_m(x,y)$ are the regression coefficients at target point. The precipitation-elevation relationship is estimated for each month and at each grid point from a weighted linear regression involving neighbouring stations. In order to take into account the influence of local surface features on precipitation distribution, the stations enter in the regression with weights depending on their nearness and orographic similarities (elevation, slope steepness, slope orientation and sea distance) to the target cell. The weighting function decay rate is locally

optimised and evaluated for each month. In particular, the radial weighting function presents an optimal halving distance ranging from about 11 km in the South during winter months to 70 km over the northernmost regions in summer.

In both MLRK and LWLR the orographic information is extracted from a smoothed version of a 1 km resolution digital elevation model (DEM). The smoothing allows to remove too fine terrain details and to consider a spatial scale more similar to that at which the interaction between atmospheric circulation and surface is expected to occur (Foresti and Pozdnoukhov, 2012). The smoothed DEM was obtained by substituting the elevation of each cell by the weighted average of the elevations of surrounding cells, with Gaussian weighting functions decreasing to 0.5 at a distance d (halving distance) from the considered cell, such that the 1 km resolution is preserved. Different halving distances were considered and d = 3 km turned out to minimize the model errors (see below for a discussion on model errors).

3.3 *Validation procedures of interpolation schemes*

The accuracy of each considered method was evaluated by reconstructing the 1981–2010 monthly precipitation normals of all the 1043 stations located in Norway. The reconstruction was performed by means of the leave-one-out (LOO) approach, i.e. by excluding the station data under estimation, in order to avoid "self-influence". In order to reduce the computational time, in the LOO procedure for all the kriging-based approaches, the covariance matrix was computed from the full database, while the kriging weight of the station to be reconstructed was set to zero and the remaining station weights renormalized. The modelled values ($\tilde{p}$) for all the N stations considered in the validation subset were compared month-by-month to the observations (p) by means of the following error estimators:

1. Mean Error (BIAS)

$$BIAS = \frac{1}{N}\sum_{i=1}^{N}(\tilde{p}_i - p_i)$$

2. Mean Absolute Error (MAE)

$$MAE = \frac{1}{N}\sum_{i=1}^{N}|\tilde{p}_i - p_i|$$

3. Mean Absolute Percentage Error (MAPE)

$$MAPE = \frac{1}{N}\sum_{i=1}^{N}\frac{|\tilde{p}_i - p_i|}{p_i}\cdot 100\%$$

4. Root Mean Squared Error (RMSE)

$$RMSE = \sqrt{\frac{1}{N}\sum_{i=1}^{N}(\tilde{p}_i - p_i)^2}$$

4. Results

4.1 *HCLIM+RK validation and comparison with observation-based methods*

The LOO errors obtained for HCLIM+RK, MLRK and LWLR 1981–2010 climatologies are shown in Table 1, together with the errors of the corresponding climatologies from the original HCLIM-AROME dataset. Thanks to the integration of in-situ observations in HCLIM+RK scheme, the significant BIAS of the original HCLIM-AROME fields is almost completely corrected in all months, especially in winter, and MAE and RMSE are reduced accordingly. The bias of the original HCLIM-AROME fields is highlighted by the distribution of the relative differences in the 1981–2010 normals between the station records and model estimates: they are shown in Figure 3 for January and July. The highest differences occur along the south-western coast and over the Lofoten islands, especially in January, where HCLIM-AROME climatologies underestimate the precipitation normals. It is worth noting that the solid precipitation undercatch, which generally affects the rain-gauge measurements depending on the intensity of snowfall events and on the site exposure to wind, could mask the actual bias of numerical model fields, whose winter precipitation underestimations could be even more relevant. In addition to the coastal bias, an overall tendency to overestimate precipitation normals occurs in July over the inland in central-southern Norway. These findings are consistent with the results obtained by Müller et al. (2017) for AROME-MetCoOp: detailed studies focusing on identifying the possible sources of AROME biases will be undertaken in the near future.

On the other hand, the BIAS is almost zero for HCLIM+RK, MLRK and LWLR, suggesting that none of the methods is affected by significant systematic errors. However, the combined HCLIM+RK approach provides the best performance in all months. The mean MAPE over all months turns out to be about 11% for HCLIM+RK and about 12% for both MLRK and LWLR. The average correlation with observations is 0.95 for HCLIM+RK and 0.94 for the other two approaches with the best agreement in winter in which HCLIM+RK reconstructions explain up to 94% of the variance of the observed station normals.

HCLIM+RK, MLRK and LWLR reconstruction errors were also evaluated for northern (above 63°18'N) and southern (below 63°18'N) Norwegian stations, separately, in order to assess the benefits provided by the integration of numerical model information where the station density is lower. In Figure 4 the resulting monthly distribution of MAE values for the three methods is reported. In both subdomains, the median is generally lower for HCLIM+RK, especially in winter, as well as the range of outliers. It is worth noting that MAPE passes on average from 10% in the South to 13% in the North for HCLIM+RK, while the increase is slightly greater for MLRK and LWLR (from 11% to 15% for both). The lower error differences between southern and northern station validations could suggest that the accuracy of the HCLIM+RK reconstruction is less influenced by the variability in data distribution over the domain.

In order to further evaluate the sensitivity of the models to data distribution, a reconstruction test was performed for southern Norway, which is the subdomain with the highest and most homogenous station coverage. The LOO normals were computed both by considering the full data availability over the subregion (728 stations) and by reducing the data density to 70% and 50%. For both data reductions, the reconstruction was iteratively performed with ten random resamples of the original station availability and the resulting errors were computed as the average of the ten simulations. Even though errors turned out to increase for all methods with reducing data coverage, the accuracy decrease obtained by using 70% and 50% of stations in comparison with the results provided by the original availability is lower for HCLIM+RK. In fact, MAPE for HCLIM+RK remains almost

invariant (about 10%) with 70% of stations and it increases to 11% with halved density, while MLRK and LWLR turn out to be more affected by the sparse station coverage with average MAPE increasing for both methods from 11% to 12% with 70% of data availability and to 14% with halved coverage. The above observations suggest that integrating in-situ information with the numerical model output could be a valuable approach to improve the robustness of reconstructed climatological fields over Norway, especially in the North where the rain-gauge network gets sparser. In these areas in fact station-based methods are forced to extrapolate precipitation gradients by means of very few and far observations and they could produce unrealistic results. On the contrary, the problem of areas scarcely covered by stations is less relevant for HCLIM+RK as observations are only used to correct model biases whose high spatial coherence allows to get reliable results even with rather low station density. HCLIM+RK climatologies have lower errors than MLRK and LWLR ones even if the HCLIM-AROME simulations on which they are based cover only a small fraction of the 1981–2010 period. The errors of HCLIM+RK estimates depend therefore both on HCLIM+RK method and on the approach we used to extend the numerical model dataset and make it representative of the 30-year reference period. The contribution of the latter factor was evaluated by means of the station records. Specifically, the monthly series of all Norwegian station sites were reconstructed over the entire period 1981–2010 by considering only the station data corresponding to the years covered by HCLIM-AROME simulations and by applying the same method used for HCLIM-AROME. The 1981–2010 station normals resulting from the reconstructed records were then compared with the corresponding observed climatologies. The results are listed in Table 2. The BIAS is almost zero in all months proving that the reconstruction procedure did not lead to systematic under- or overestimations, while correlation between estimated and observed monthly normals is always greater than 0.99. RMSE and MAPE, as averages over the months, are 4.3 mm and 3.3%, respectively, suggesting that the errors due to the reconstruction of missing data can be considered rather low in comparison with those ascribing to HCLIM+RK method. The small influence of the missing data period simulation on the HCLIM+RK accuracy can be explained by the fact that the reconstruction

306 procedure is equivalent to multiplying the 2003–2016 climatologies by the ratio between the 1981–
307 2010 and 2003–2016 normals of surrounding stations and this ratio shows a very high spatial
308 coherence over the domain in all months. The distribution of this ratio for January and July at all
309 station sites is reported in Figure 5. The sites showing values strongly deviating from those of the
310 neighbouring sites are more likely to be affected by inhomogeneities in their records than to represent
311 actual outliers in climatological ratio.
312 The low errors provided by the extension of the 2003–2016 model records to the 1980–2010 window
313 indicate that the same method we used to get the 1981–2010 climatologies could be applied also over
314 other previous 30-year periods (e.g. 1971–2000, 1961–1990), even though the errors are expected to
315 increase due to the lack of overlapping years of data and to the increasing probability of break
316 occurrences in station records.
317 Furthermore, the above findings prove the relative low contribution of missing period reconstruction
318 on the errors of 1981–2010 HCLIM+RK climatologies; however, they also suggest that the accuracy
319 of the interpolation method is not expected to sharply improve even with the availability of numerical
320 model simulations over a longer period.
321 In addition to the model comparison by station validation, HCLIM+RK results were compared with
322 the output of MLRK and LWLR also at grid point level in order to detect the specific features of the
323 continuous precipitation field provided by the different approaches. In Figures 6 and 7 the differences
324 of MLRK and LWLR gridded monthly precipitation climatologies for January (a) and July (b) with
325 respect to HCLIM+RK fields are reported. Both models show an overall tendency to underestimate
326 winter precipitation especially along the coastal reliefs throughout the country, with the lowest
327 estimates at the highest elevated grid points. On average, MLRK and LWLR precipitation normals in
328 January are lower than HCLIM+RK values of about 20 mm in northern Norway and of about 7 and
329 11 mm, respectively, in the South. However, if only points above 800 m a.s.l. are considered, the
330 mean underestimation increases for both methods with the most negative discrepancies for LWLR in
331 both subregions. As regards July normals, the discrepancies with HCLIM+RK are more spatially

heterogeneous for both methods and relevant discontinuities are evident, especially in the LWLR climatology over central Norway where negative biases turn into relevant overestimations within very short distances. The drying tendency and wet outliers mostly occur over the lowest sampled areas where the local available information used in MLRK and LWLR interpolation is not enough to model reliable precipitation gradients. This is particularly evident if the discrepancies with HCLIM+RK output are clustered for elevation ranges (Figure 8). In January they turn out to gradually increase with elevation for both MLRK and LWLR which could be a consequence of the decrease in data availability over the mountainous regions. The distribution of discrepancies for July does not show a significant trend over elevation ranges below 1200 m a.s.l. and the medians for MLRK and LWLR are almost comparable. At the grid cells above 1200 m a.s.l. (about 8% of the total) MLRK and LWLR provide on average higher July normals than HCLIM+RK and this discrepancy could be partly due to the original negative bias affecting the HCLIM-AROME summer precipitation fields (Figure 3b) over the mountainous coastal regions not completely corrected by the RK on station data. In both months the interquartile ranges and extremes of outliers are generally greater for LWLR suggesting a major instability of its modelled fields. Moreover, the LWLR discrepancies are expected to be even greater. In fact over the least sampled areas this method reconstructed some negative precipitation, which was automatically corrected within the algorithm by substituting the regression with a simple weighted average based on station distance. This correction could be suitable for adjusting single points, whereas it could give rise to evident discontinuities when the extent of negative precipitation areas gets wider. LWLR negative estimates are mostly likely to occur if no significant elevation gradients exist at the target cell and/or if the uneven station distribution leads to misjudge the local precipitation-elevation relationship. This problem is partly reduced in MLRK thanks to the inclusion of more geographical predictors and to the larger spatial scales considered in the interpolation, however some isolated and slightly negative normals still occur for some months.

The above findings suggest that the interpolated climatologies provided by the observation-based methods are more likely to be affected by discontinuities and outliers where the station coverage gets

sparser and pure extrapolation is performed, whereas the integration of numerical model fields into the HCLIM+RK procedure could help to reconstruct more stable precipitation gradients and to reduce the underestimation of winter normals over the highest elevated areas of Norway.

4.2 *HCLIM+RK 1981–2010 monthly precipitation climatologies over Norway*

According to the results discussed in the above section we selected the HCLIM+RK as the reference climatology for Norway and we analysed it to assess the spatial distribution of precipitation over the country. The HCLIM+RK seasonal and annual precipitation climatologies for the period 1981–2010 are presented in Figures 9 and 10, respectively. The average seasonal precipitation normals (winter, spring, summer and autumn) over the whole domain are 339, 220, 263 and 364 mm, respectively, while the average annual precipitation is 1186 mm. The mean precipitation totals reconstructed by MLRK on both seasonal and annual scales are in agreement with HCLIM+RK results (correlation values always above 0.9) even if they are underestimated in all cases of about 10% with respect to the HCLIM+RK reference values.

The spatial distribution of HCLIM+RK precipitation climatologies is mainly dominated by a strong and well-defined West-to-East gradient along the whole country in all seasons, with the highest normals in correspondence to the coastal reliefs, acting as orographic barrier to the wet air masses from the sea, and a quick transition to rather dry conditions over the leeward side and inland. The wettest area in Norway is located around the Ålfotbreen glacier (1385 m), near the Nordfjorden. The mean annual precipitation over this area exceeds 5700 mm with the greatest contributions from winter precipitation, accounting for more than 30% of annual totals. This value is in agreement with the measures performed by the Norwegian Water Resources and Energy Directorate (NVE) of snow accumulation length over the glacier during the winter season and drainage from river basins which indicate that annual precipitation (normal period 1961-1990) for the area are greater than 5500 mm (Teigen, 2005). Another very wet region is depicted around the Svartisen glacier in northern Norway with annual precipitation values around 3000 mm. On the contrary the driest conditions occur

between Otta and Gudbrand Valleys, located on the bottom of the leeward side of the West mountain chain, where the absolute minimum annual normal is reconstructed (243 mm).

Furthermore, precipitation is found to reduce significantly also towards the northernmost part of the country, where the annual normals decrease below 300 mm, especially over Finnmark. It is worth noting that over northern Norway the expected positive precipitation gradient moving from the flat regions of inland to the more mountainous coastal areas is depicted along the whole year. This gradient is reconstructed thanks to the background information supplied by HCLIM-AROME numerical model fields, while it is not captured or turns negative if only in-situ observations enter into the climatological computation, as in MLRK and LWLR, whose extrapolation over under-sampled areas leads to underestimations in most cases. By taking into account the grid cells above 69°N and 500 m a.s.l. only, the average annual precipitation in HCLIM+RK climatology is in fact about 300 mm higher than in MLRK and, except for summer, the HCLIM+RK seasonal precipitation normals are almost twice greater than MLRK estimates.

Further interesting information about Norwegian climate can be retrieved from the distribution of annual precipitation cycles over the country (Figure 11). The average yearly patterns were computed over consecutive 10000 km^2 areas covering the whole domain, after filtering the normal cycle of each grid point by means of a trigonometric function in order to reduce the discontinuities from one month to another. All the Norwegian subregions which are close to the sea experience the highest relative monthly contributions to annual precipitation in winter and the lowest ones in late spring or summer and this annual pattern turns out to be almost constant with latitude. Moving from the coast towards the inland, the climate turns to be characterised by maximum precipitation in summer and minimum in winter or early spring. Moreover, the relative contributions of summer precipitation to the annual cycles over the inner areas increase towards the North of about 3%, except for the northernmost subregions where the very dry conditions lead to more homogeneous precipitation regimes along the year and slightly higher contributions in late summer and autumn. Also the area around Oslo Fjord

on the southern coast experiences a more smoothed yearly cycle with the main contributions in late summer when the convective phenomena prevail.

In Figure 11, the annual cycles over the considered subregions are superimposed on the spatial distribution of the ratio between winter and summer precipitation normals at each point of the 1 km grid. It confirms the existence of two main distinctive climatic regimes with the prevalence of orographic enhancement mechanisms for precipitation over the mountainous coast and of more continental conditions over the inland. More specifically, the winter to summer precipitation ratio ranges on average between 1.5 and 3 over the coastal Norway, with the greatest values over the highest areas, whereas the ratio is below unity over the inland where summer precipitation normals become twice the winter ones for a large fraction of grid cells. In addition, it is worth noting the occurrence of a "transition zone" crossing the whole country from North to South characterised by quite comparable contributions of winter and summer precipitation amounts.

5. Conclusions

The 1981–2010 monthly precipitation climatologies over Norway were computed at 1 km resolution by applying a new combined interpolation approach, named HCLIM+RK. The method joins a database of quality-checked rain-gauge observations with the 1981–2010 monthly precipitation fields derived from the 2003–2016 reanalysis driven regional climate HCLIM-AROME model at 2.5 km resolution.

The ability of this approach to deal with the uneven data coverage of Norway and to provide reliable precipitation patterns also where station density gets lower was evaluated by the comparison with two interpolation schemes using only observations: MLRK and LWLR.

HCLIM+RK turned out to provide the lowest errors in reconstructing the station normals in all months with MAPE ranging from 8.7% (September) to 13.5% (March). Moreover, the significant biases affecting HCLIM-AROME numerical model fields were almost removed thanks to the integration with station observations. The better performance of HCLIM+RK are also evident if the reconstruction is evaluated on northern and southern stations, separately. MLRK and LWLR provide

higher errors and larger ranges of outliers, especially in the North where the network is sparser, suggesting the greater influence of the variation in data availability on their accuracy. A sensitivity test was also performed on the three methods and it confirmed the greater stability of HCLIM+RK results with varying station distribution and density. The reconstruction errors of HCLIM+RK remained almost unaltered by reducing the data availability, while MLRK and LWLR errors increased more significantly.

By comparing the gridded precipitation climatologies for January and July, MLRK and LWLR showed systematic underestimations over coastal regions with respect to HCLIM+RK reconstruction, especially in winter with increasing grid cell elevation. In addition, the observation-based models are affected by relevant spatial discontinuities in precipitation distribution and some negative estimates also occur, especially for LWLR, where the rain-gauge coverage is sparser.

The contribution to the global HCLIM+RK errors provided by extrapolating the 1981–2010 normals from the 2003–2016 HCLIM-AROME fields was also evaluated by simulating the same reconstruction approach on station data. The series reconstruction provided much lower errors than those of the whole HCLIM+RK procedure (average MAPE was 3% and 11%, respectively) and the overall coherence in climatological ratios among stations proved the robustness of HCLIM-AROME run extension.

The HCLIM+RK precipitation climatologies for the period 1981–2010 are characterised by a sharp West-to-East transition from the wet mountainous coast, which is interested by orographic precipitation regime, to the drier inland experiencing more continental climate.

Even if the precipitation normals decrease significantly in the northernmost part of Norway, a positive gradient with elevation is preserved thanks to the information provided by HCLIM-AROME numerical fields. The total lack of observations at the high-elevated areas of northern Norway leads in fact the observation-based approaches to mainly extrapolate decreasing precipitation with altitude.

458 The distributions of annual cycles as well as of the winter-to-summer ratios obtained from
459 HCLIM+RK climatologies confirm the main precipitation gradients over the country and depict the
460 more specific climatic features of the different subregions.
461 The presented findings prove that the interpolation approach combining numerical model information
462 with in-situ observations allows to better deal with the uneven station network over Norway and to
463 significantly increase the accuracy of resulting climatologies, especially over the most remote
464 regions. Future analyses aiming at identifying the sources of numerical model biases as well as the
465 integration of the most recent automatic station observations at remote sites could help to further
466 increase the accuracy of the available monthly precipitation climatologies over the country.

467 **7. Acknowledgments**

468 The authors thank the Norwegian Meteorological Institute and the European Climate Assessment &
469 Dataset project whose data contributed to set up the 1981–2010 precipitation database used in the
470 present work. We also thank the MET Climate Division for providing the HCLIM-AROME climate
471 simulations and the precious suggestion to correctly manage the numerical model dataset.
472 Computational and storage resources for the simulations have been provided by the European Centre
473 for Medium-Range Weather Forecasts (ECMWF) and UNINETT Sigma2-the National Infrastructure
474 for High Performance Computing and Data Storage in Norway. The modelers would also like to thank
475 The Research Council of Norway for funding of the simulations within the WISLINE project. The
476 complete model dataset is freely available at
477 http://thredds.met.no/thredds/catalog/metusers/andreasd/WISLINE_HCLIM_NORWAY/catalog.ht
478 ml.

479 **References**

480 Berthou, S., Kendon, E. J., Chan, S. C., Ban, N., Leutwyler, D., Schär, C., & Fosser, G. (2018). Pan-
481 European climate at convection-permitting scale: a model intercomparison study. Climate Dynamics.
482 https://doi.org/10.1007/s00382-018-4114-6

Boer, E. P. J., De Beurs, K. M., & Hartkamp, A. D. (2001). Kriging and thin plate splines for mapping climate variables. International Journal of Applied Earth Observation and Geoinformation, 3, 146–154. https://doi.org/10.1016/S0303-2434(01)85006-6

Crespi, A., Brunetti, M., Lentini, G., & Maugeri, M. (2018). 1961-1990 high-resolution monthly precipitation climatologies for Italy. International Journal of Climatology, 38, 878–895. https://doi.org/10.1002/joc.5217

Daly, C., Gibson, W. P., Taylor, G. H., Johnson, G. L., & Pasteris, P. (2002). A knowledge based approach to the statistical mapping of climate. Climate Research, 22, 99–113. www.jstor.org/stable/24868310

Daly, C., Halbleib, M., Smith, J. I., Gibson, W. P., Doggett, M. K., Taylor, G. H., Curtis, J., & Pasteris, P. A. (2008). Physiographically-sensitive mapping of temperature and precipitation across the conterminous United States. International Journal of Climatology, 28, 2031–2064. https://doi.org/10.1002/joc.1688

Dee, D. P., Uppala, S. M., Simmons, A. J., Berrisford, P., Poli, P., Kobayashi, S., Andrae, U., Balmaseda, M. A., Balsamo, G., Bauer, D. P., & Bechtold, P. (2011). The ERA-Interim reanalysis: Configuration and performance of the data assimilation system. Quarterly Journal of the Royal Meteorological Society, 137(656), 553–597. https://doi.org/10.1002/qj.828

Dyrrdal, A. V., Stordal, F., & Lussana, C. (2018). Evaluation of summer precipitation from EURO-CORDEX fine-scale RCM simulations over Norway. International Journal of Climatology, 38, 1661–1677. https://doi.org/10.1002/joc.5287

Dyrrdal A. V., Lenkoski A., Thorarinsdottir T. L., & Stordal F. (2015). Bayesian hierarchical modeling of extreme hourly precipitation in Norway. Environmetrics, 26, 89–106. https://doi.org/10.1002/env.2301

Foresti, L., & Pozdnoukhov, A. (2012). Exploration of alpine orographic precipitation patterns with radar image processing and clustering techniques. Meteorological Applications, 19, 407–419. https://doi.org/10.1002/met.272

509 Golzio, A., Crespi, A., Bollati, I. M., Senese, A., Diolaiuti, G. A., Pelfini, M., & Maugeri, M. (2018).
510 High-Resolution Monthly Precipitation Fields (1913–2015) over a Complex Mountain Area Centred
511 on the Forni Valley (Central Italian Alps). Advances in Meteorology, 2018, ID 9123814, pp. 17.
512 https://doi.org/10.1155/2018/9123814
513 Goovaerts, P. (2000). Geostatistical approaches for incorporating elevation into the spatial
514 interpolation of rainfall. Journal of Hydrology, 228, 113–129. https://doi.org/10.1016/S0022-
515 1694(00)00144-X
516 Haylock, M. R., Hofstra, N., Klein Tank, A. M. G., Klok, E. J., Jones, P. D., & New, M. (2008). A
517 European daily high-resolution gridded data set of surface temperature and precipitation for 1950–
518 2006. Journal of Geophysical Research, 113, D20119. https://doi.org/10.1029/2008JD010201
519 Hengl, T. (2009). A Practical Guide to Geostatistical Mapping, ISBN 978-90-9024981-0. Licensed
520 under a creative Commons Attribution-Noncommercial-No Derivative Works 3.0 license. Available
521 at http://spatial-analyst.net/book/.
522 Henn, B., Newman A. J., Livneh, B., Daly, C., & Lundquist, J. D. (2018). An assessment of
523 differences in gridded precipitation datasets in complex terrain. Journal of Hydrology, 556, 1205–
524 1219. https://doi.org/10.1016/j.jhydrol.2017.03.008
525 Isotta, F., Vogel, R., & Frei, C. (2015). Evaluation of European regional reanalyses and downscalings
526 for precipitation in the Alpine region. Meteorologische Zeitschrift, 24, 15–37.
527 https://doi.org/10.1127/metz/2014/0584
528 Jermey, P. M., & Renshaw, R. J. (2016). Precipitation representation over a two-year period in
529 regional reanalysis. Quarterly Journal of the Royal Meteorological Society, 142, 1300–1310.
530 https://doi.org/ https://doi.org/10.1002/qj.2733
531 Karger, D. N., Conrad, O., Böhner, J., Kawohl, T., Kreft, H., Soria-Auza, R. W., Zimmermann, N.
532 E., Linder, H. P., & Kessler, M. (2017). Climatologies at high resolution for the earth's land surface
533 areas. Scientific Data, 4: 170122. https://doi.org/10.1038/sdata.2017.122

534 Lind, P., Lindstedt, D., Kjellström, E., & Jones, C. (2016). Spatial and temporal characteristics of
535 summer precipitation over central europe in a suite of high-resolution climate models. Journal of
536 Climate, 29(10), 3501–3518. https://doi.org/10.1175/JCLI-D-15-0463.1
537 Lussana, C., Saloranta, T., Skaugen, T., Magnusson, J., Tveito, O. E., & Andersen, J. (2018).
538 seNorge2 daily precipitation, an observational gridded dataset over Norway from 1957 to the present
539 day. Earth System Science Data, 10, 235–249. https://doi.org/10.5194/essd-10-235-2018
540 Masson, V., Le Moigne, P., Martin, E., Faroux, S., Alias, A., Alkama, R., … & Voldoire, A. (2013).
541 The surfexv7.2 land and ocean surface platform for coupled or offline simulation of earth surface
542 variables and fluxes. Geoscientific Model Development, 6, 929–960. https://doi.org/10.5194/gmd-6-
543 929-2013
544 Mohr, M. (2008). New routines for gridding of temperature and precipitation observations for
545 "seNorge. no", Met. no Report, 8, the Norwegian Meteorological Institute, Oslo, Norway.
546 Mohr, M. (2009). Comparison of versions 1.1 and 1.0 of gridded temperature and precipitation data
547 for Norway, Norwegian Meteorological Institute, met no note, 19, the Norwegian Meteorological
548 Institute, Oslo, Norway.
549 Müller, M., Homleid, M., Ivarsson, K., Køltzow, M. A., Lindskog, M., Midtbø, K. H., Andrae, U.,
550 Aspelien, T., Berggren, L., Bjørge, D., Dahlgren, P., Kristiansen, J., Randriamampianina, R., Ridal,
551 M., & Vignes, O. (2017). AROME-MetCoOp: A Nordic Convective-Scale Operational Weather
552 Prediction Model. Weather and Forecasting, 32, 609–627. https://doi.org/10.1175/WAF-D-16-
553 0099.1
554 Prein, A. F., & Gobiet, A. (2017). Impacts of uncertainties in European gridded precipitation
555 observations on regional climate analysis. International Journal of Climatology, 37, 305–327.
556 https://doi.org/10.1002/joc.4706
557 Seity, Y., Brousseau, P., Malardel, S., Hello, G., Bénard, P., Bouttier, F., Lac, C., & Masson, V.
558 (2011). The AROME-France Convective-Scale Operational Model, Monthly Weather Review, 139,
559 976–991. https://doi.org/10.1175/2010MWR3425.1

560 Simmons, A. J., Berrisford, P., Dee, D. P., Hersbach, H., Hirahara, S., & Thépaut, J. (2017). A
561 reassessment of temperature variations and trends from global reanalyses and monthly surface
562 climatological datasets. Quarterly Journal of the Royal Meteorological Society, 143, 101–119.
563 https://doi.org/10.1002/qj.2949
564 Teigen, R. (2005). Numerical simulation of orographic precipitation in western Norway. Master
565 degree thesis, Geophysical Institute, University of Bergen (in Norwegian).
566 http://hdl.handle.net/1956/1296
567 Tveito, O. E., Bjørdal, I., Skjelvåg, A. O., & Aune, B. (2005). A GIS-based agro-ecoglogical decision
568 system based on gridded climatology. Meteorological Applications, 12, 57–68,
569 https://doi.org/10.1017/S1350482705001490

	HCLIM-AROME			HCLIM+RK				MLRK				LWLR			
	BIAS	MAE	RMSE	BIAS	MAE	MAPE [%]	RMSE	BIAS	MAE	MAPE [%]	RMSE	BIAS	MAE	MAPE [%]	RMSE
1	-18.3	26.0	36.9	0.3	13.9	12.5	21.2	0.6	15.9	14.4	25.1	-0.1	16.5	14.3	26.4
2	-14.0	20.3	29.0	0.2	11.3	13.4	17.5	0.5	12.9	15.3	20.3	-0.3	13.4	15.2	21.2
3	-13.5	20.6	29.4	0.2	10.4	13.5	15.9	0.4	12.1	15.5	18.9	-0.2	12.5	15.4	19.8
4	-5.1	14.8	19.7	0.1	7.3	12.9	10.8	0.2	8.4	14.7	12.9	-0.3	8.6	14.4	13.1
5	-0.1	12.0	15.9	0.1	6.3	10.4	9.2	0.0	7.0	11.5	10.8	-0.4	7.0	11.3	10.4
6	-3.4	16.6	21.2	0.0	6.9	9.9	9.6	0.0	7.1	10.1	10.7	-0.3	7.2	10.0	10.5
7	-0.9	20.1	26.2	0.1	7.9	9.1	11.2	0.0	7.8	8.9	11.7	-0.1	7.8	8.8	11.8
8	-7.1	22.9	29.6	0.1	9.0	8.9	12.9	0.0	9.5	9.2	14.6	-0.3	9.7	9.2	14.7
9	-21.3	27.4	38.8	0.2	10.3	8.7	16.2	0.1	12.4	10.7	20.4	-0.3	12.5	10.3	20.0
10	-26.4	31.1	42.0	0.2	12.2	9.4	18.8	0.3	14.3	11.3	22.9	-0.3	14.6	11.1	22.8
11	-20.9	28.0	37.9	0.3	11.8	11.0	18.4	0.5	13.9	12.9	21.7	-0.1	14.1	12.6	22.0
12	-20.6	26.5	36.8	0.2	13.1	12.2	20.3	0.5	15.1	14.0	24.2	-0.3	15.5	13.9	24.8

Table 1: Monthly leave-one-out reconstruction errors of HCLIM+RK, MLRK and LWLR for the 1043 Norwegian stations together with the errors of the 1981–2010 monthly normals from HCLIM-AROME original fields. Except for MAPE, all the values are expressed in mm and BIAS is defined as the difference between simulation and observation.

	1981–2010 station simulation			
	BIAS	MAE	MAPE [%]	RMSE
1	0.1	3.7	3.5	5.6
2	0.2	3.4	4.1	5.3
3	0.1	3.0	4.1	4.6
4	0.1	2.2	3.8	3.2
5	0.0	1.9	3.1	2.7
6	0.1	2.2	3.1	3.0
7	0.0	2.7	3.0	3.7
8	0.1	3.2	3.2	4.5
9	0.1	3.0	2.8	4.3
10	0.0	3.4	2.8	5.0
11	0.0	3.2	2.9	4.7
12	0.0	3.6	3.5	5.4
MEAN	**0.1**	**3.0**	**3.3**	**4.3**

Table 2: Errors of the 1981–2010 monthly precipitation normals computed from the simulated records of the 1043 Norwegian stations. Except for MAPE, all the values are expressed in mm and BIAS is defined as the difference between simulation and observation.

CAPTIONS OF TABLES AND FIGURES

Figure 1: Distribution of the 2009 stations considered for the Norwegian climatology reconstruction.

Figure 2: Vertical distribution of the 1043 Norwegian stations (red solid line) compared to the grid-cell elevation distribution (blue dashed line) over Norway.

Table 1: Monthly leave-one-out reconstruction errors of HCLIM+RK, MLRK and LWLR for the 1043 Norwegian stations together with the errors of the 1981–2010 monthly normals from HCLIM-AROME original fields. Except for MAPE, all the values are expressed in mm and BIAS is defined as the difference between simulation and observation.

Figure 3: Distribution over Norway of the relative BIAS [%] of HCLIM-AROME dataset for a) January and b) July. The values are obtained by comparing the 1981–2010 monthly climatologies of

HCLIM-AROME with the station normals and by normalising the differences for the average of numerical model and rain-gauge values.

Figure 4: Monthly MAE distribution of the reconstructed normals by the three methods for stations located in a) northern Norway (above 63°18'N) and b) southern Norway (below 63°18'N). The boxes represent the inter-quartile range of the distribution where the median is reported by the bold line; the whiskers represent the 5–95% quantile range.

Figure 5: Distribution of the ratios between the 1981–2010 and 2003–2016 normals of all the stations in the database for a) January and b) July.

Table 2: Errors of the 1981–2010 monthly precipitation normals computed from the simulated records for the 1043 Norwegian stations. Except for MAPE, all the values are expressed in mm and BIAS is defined as the difference between simulation and observation.

Figure 6: Discrepancies of a) MLRK and b) LWLR with HCLIM+RK in 1981–2010 gridded precipitation climatologies for January.

Figure 7: Discrepancies of a) MLRK and b) LWLR with HCLIM+RK in 1981–2010 gridded precipitation climatologies for July.

Figure 8: Distribution of MLRK and LWLR discrepancies with HCLIM+RK gridded a) January and b) July climatologies on elevation ranges. The boxes represent the inter-quartile range of the distribution where the median is reported by the bold line; the whiskers represent the 5–95% quantile range.

Figure 9: Seasonal HCLIM+RK precipitation climatologies.

Figure 10: Annual HCLIM+RK precipitation climatology.

Figure 11: Distribution of winter (DJF) to summer (JJA) precipitation ratio over the domain and of the average yearly precipitation cycles over different 10000 km^2 subdomains covering Norway. The

inset box defines the range of axes that is the same for all the plots. The values are expressed as percentage to the total annual precipitation.

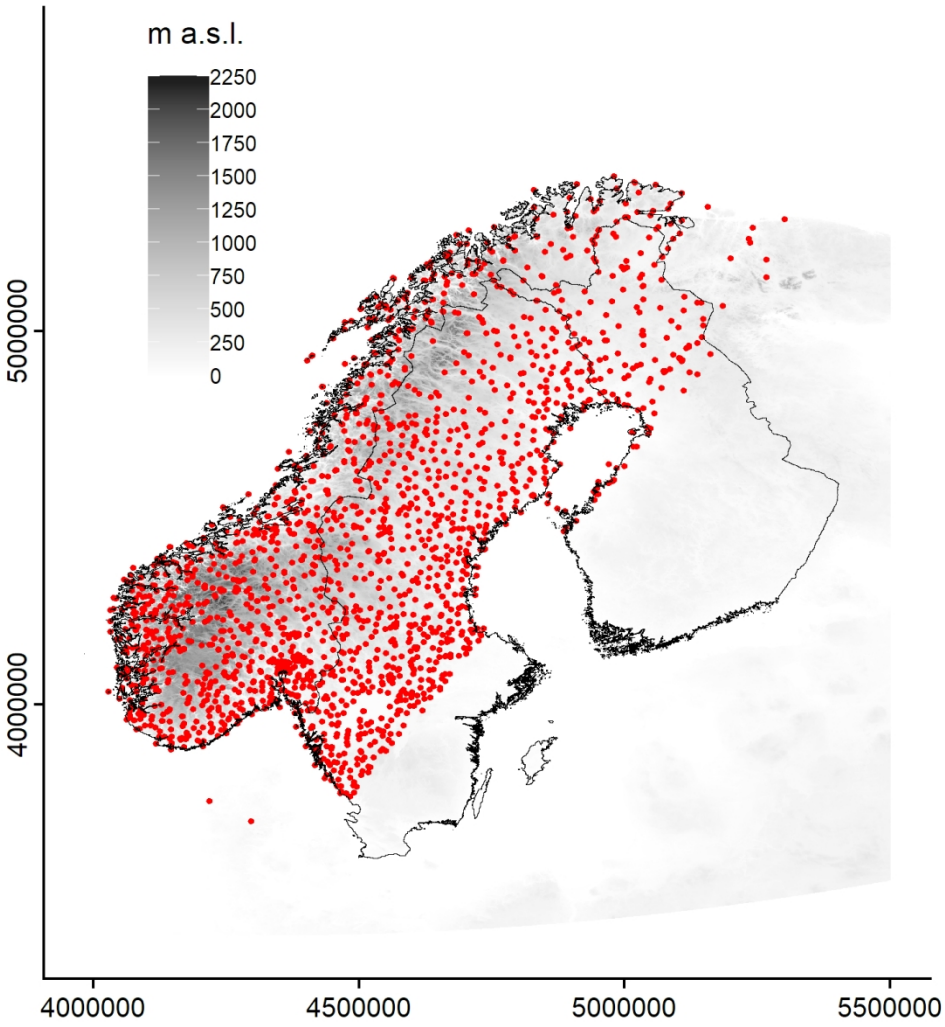

Distribution of the 2009 stations considered for the Norwegian climatology reconstruction.

129x139mm (300 x 300 DPI)

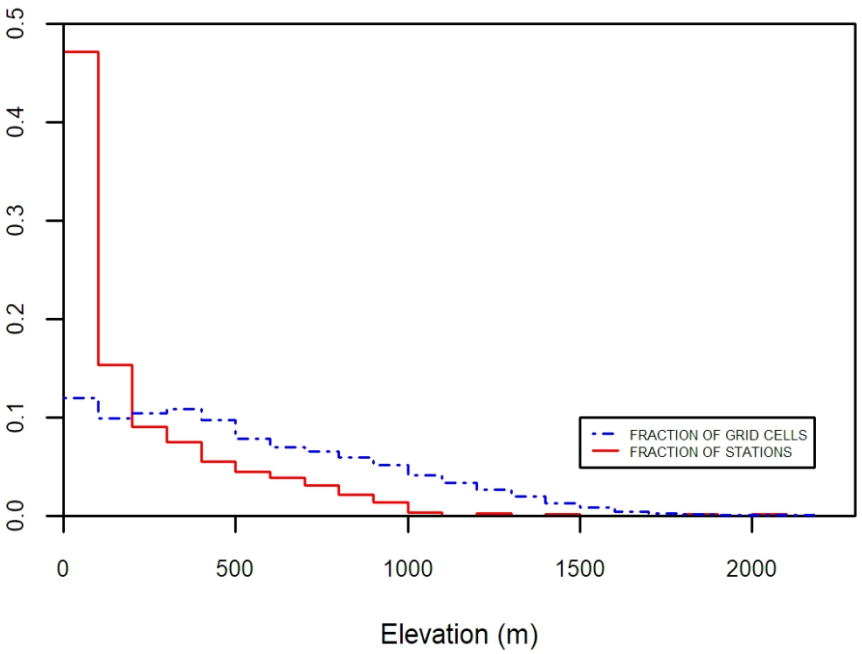

Vertical distribution of the 1043 Norwegian stations (red solid line) compared to the grid-cell elevation distribution (blue dashed line) over Norway.

99x79mm (300 x 300 DPI)

	HCLIM-AROME			HCLIM+RK				MLRK				LWLR			
	BIAS	MAE	RMSE	BIAS	MAE	MAPE [%]	RMSE	BIAS	MAE	MAPE [%]	RMSE	BIAS	MAE	MAPE [%]	RMSE
1	-18.3	26.0	36.9	0.3	13.9	12.5	21.2	0.6	15.9	14.4	25.1	-0.1	16.5	14.3	26.4
2	-14.0	20.3	29.0	0.2	11.3	13.4	17.5	0.5	12.9	15.3	20.3	-0.3	13.4	15.2	21.2
3	-13.5	20.6	29.4	0.2	10.4	13.5	15.9	0.4	12.1	15.5	18.9	-0.2	12.5	15.4	19.8
4	-5.1	14.8	19.7	0.1	7.3	12.9	10.8	0.2	8.4	14.7	12.9	-0.3	8.6	14.4	13.1
5	-0.1	12.0	15.9	0.1	6.3	10.4	9.2	0.0	7.0	11.5	10.8	-0.4	7.0	11.3	10.4
6	-3.4	16.6	21.2	0.0	6.9	9.9	9.6	0.0	7.1	10.1	10.7	-0.3	7.2	10.0	10.5
7	-0.9	20.1	26.2	0.1	7.9	9.1	11.2	0.0	7.8	8.9	11.7	-0.1	7.8	8.8	11.8
8	-7.1	22.9	29.6	0.1	9.0	8.9	12.9	0.0	9.5	9.2	14.6	-0.3	9.7	9.2	14.7
9	-21.3	27.4	38.8	0.2	10.3	8.7	16.2	0.1	12.4	10.7	20.4	-0.3	12.5	10.3	20.0
10	-26.4	31.1	42.0	0.2	12.2	9.4	18.8	0.3	14.3	11.3	22.9	-0.3	14.6	11.1	22.8
11	-20.9	28.0	37.9	0.3	11.8	11.0	18.4	0.5	13.9	12.9	21.7	-0.1	14.1	12.6	22.0
12	-20.6	26.5	36.8	0.2	13.1	12.2	20.3	0.5	15.1	14.0	24.2	-0.3	15.5	13.9	24.8

Table 1: Monthly leave-one-out reconstruction errors of HCLIM+RK, MLRK and LWLR for the 1043 Norwegian stations together with the errors of the 1981–2010 monthly normals from HCLIM-AROME original fields. Except for MAPE, all the values are expressed in mm and BIAS is defined as the difference between simulation and observation.

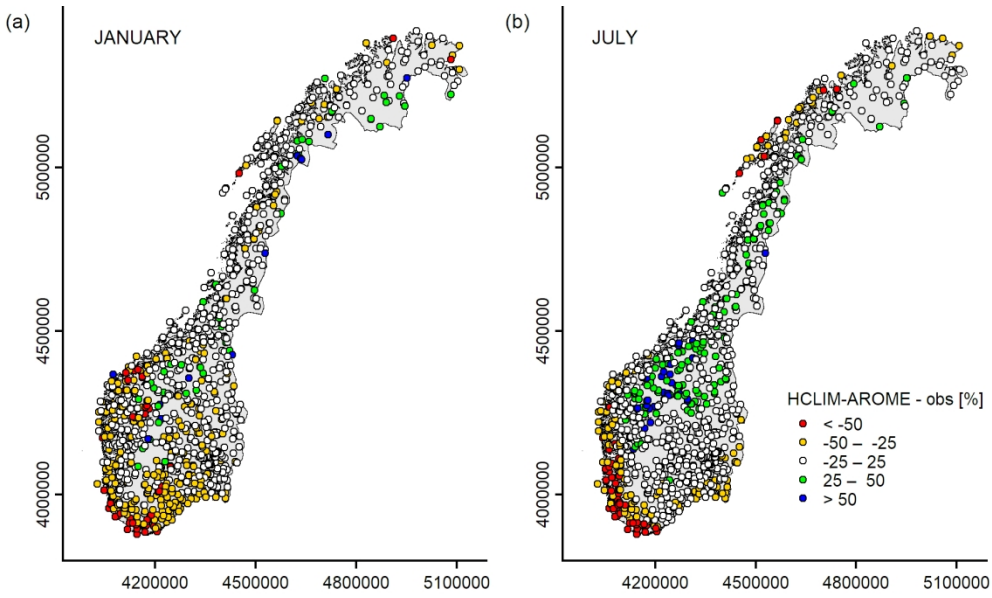

Distribution over Norway of the relative BIAS [%] of HCLIM-AROME dataset for a) January and b) July. The values are obtained by comparing the 1981–2010 monthly climatologies of HCLIM-AROME with the station normals and by normalising the differences for the average of numerical model and rain-gauge values.

159x99mm (300 x 300 DPI)

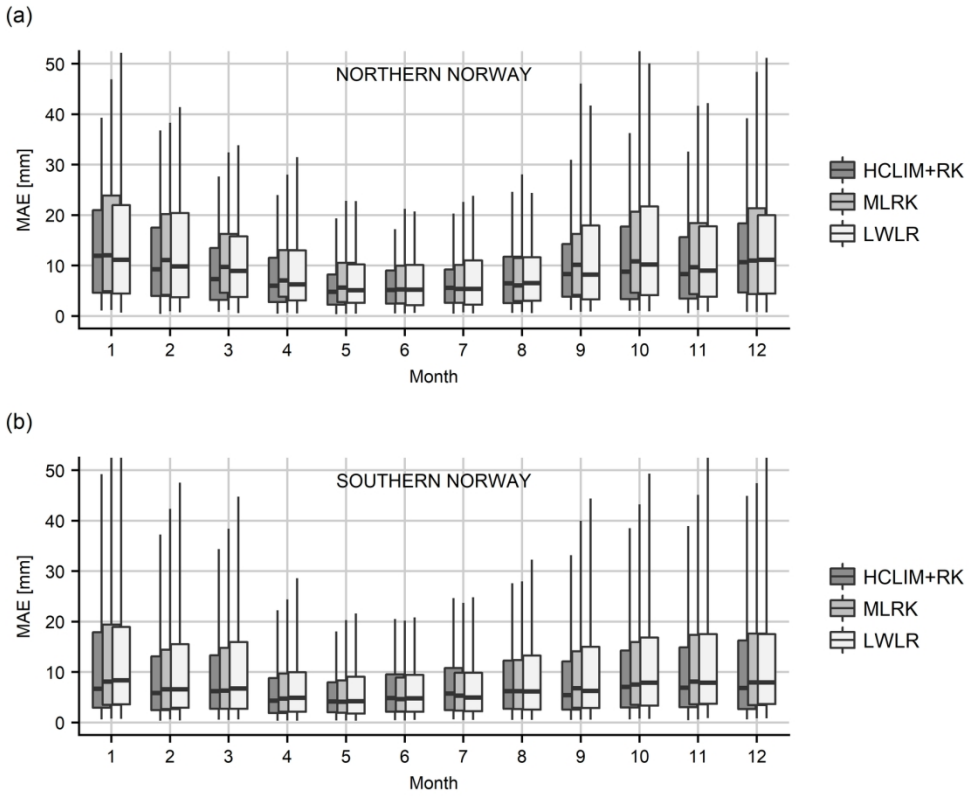

Monthly MAE distribution of the reconstructed normals by the three methods for stations located in a) northern Norway (above 63°18′N) and b) southern Norway (below 63°18′N). The boxes represent the inter-quartile range of the distribution where the median is reported by the bold line; the whiskers represent the 5–95% quantile range.

159x129mm (300 x 300 DPI)

	1981–2010 station simulation			
	BIAS	MAE	MAPE [%]	RMSE
1	0.1	3.7	3.5	5.6
2	0.2	3.4	4.1	5.3
3	0.1	3.0	4.1	4.6
4	0.1	2.2	3.8	3.2
5	0.0	1.9	3.1	2.7
6	0.1	2.2	3.1	3.0
7	0.0	2.7	3.0	3.7
8	0.1	3.2	3.2	4.5
9	0.1	3.0	2.8	4.3
10	0.0	3.4	2.8	5.0
11	0.0	3.2	2.9	4.7
12	0.0	3.6	3.5	5.4
MEAN	**0.1**	**3.0**	**3.3**	**4.3**

Table 2: Errors of the 1981–2010 monthly precipitation normals computed from the simulated records of the 1043 Norwegian stations. Except for MAPE, all the values are expressed in mm and BIAS is defined as the difference between simulation and observation.

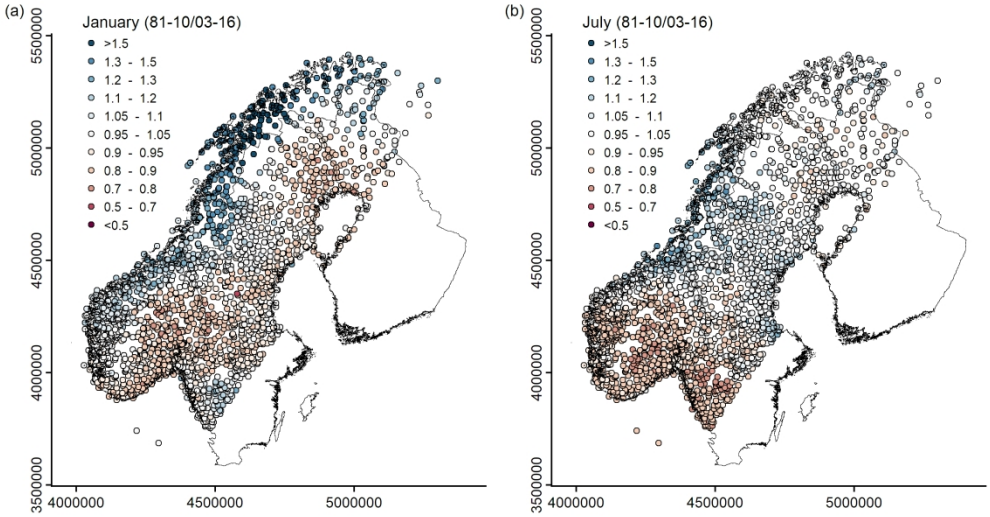

Distribution of the ratios between the 1981–2010 and 2003–2016 normals of all the stations in the database for a) January and b) July.

219x119mm (300 x 300 DPI)

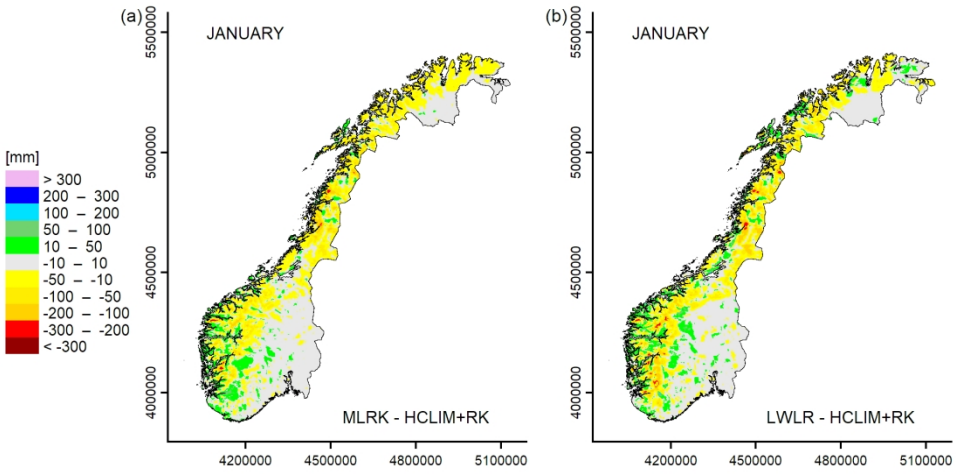

Discrepancies of a) MLRK and b) LWLR with HCLIM+RK in 1981–2010 gridded precipitation climatologies for January.

179x89mm (300 x 300 DPI)

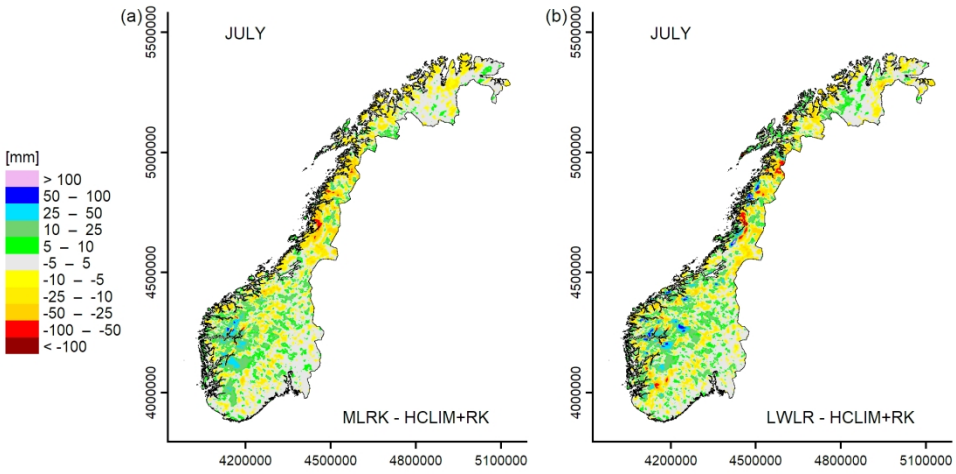

Discrepancies of a) MLRK and b) LWLR with HCLIM+RK in 1981–2010 gridded precipitation climatologies for July.

179x89mm (300 x 300 DPI)

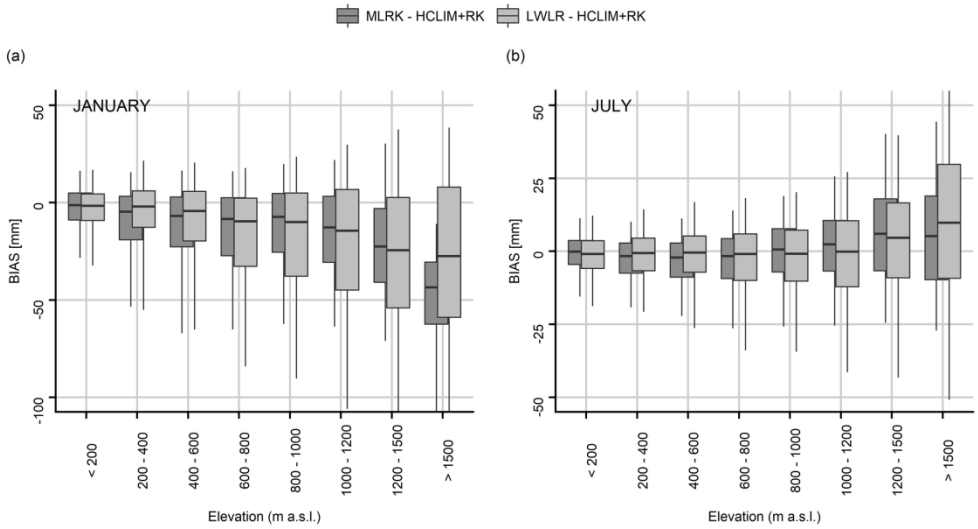

Distribution of MLRK and LWLR discrepancies with HCLIM+RK gridded a) January and b) July climatologies on elevation ranges. The boxes represent the inter-quartile range of the distribution where the median is reported by the bold line; the whiskers represent the 5–95% quantile range.

179x99mm (300 x 300 DPI)

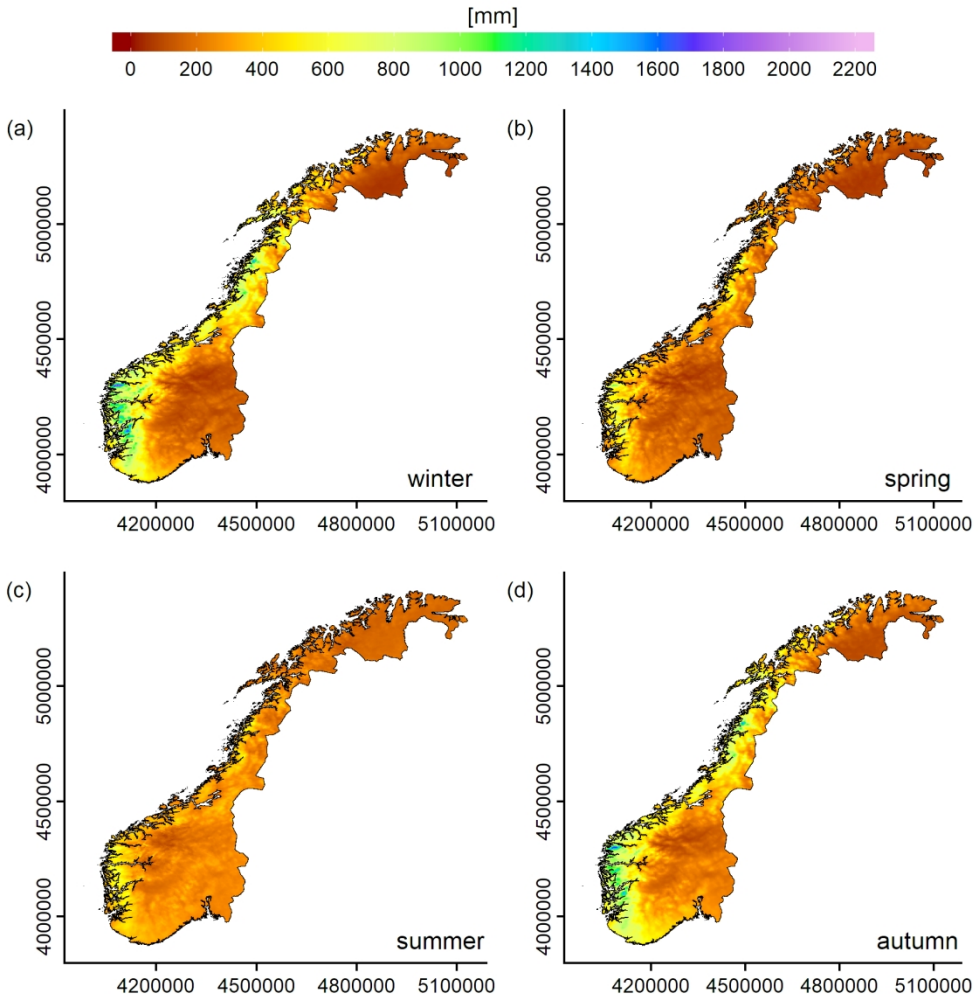

Seasonal HCLIM+RK precipitation climatologies.

159x169mm (300 x 300 DPI)

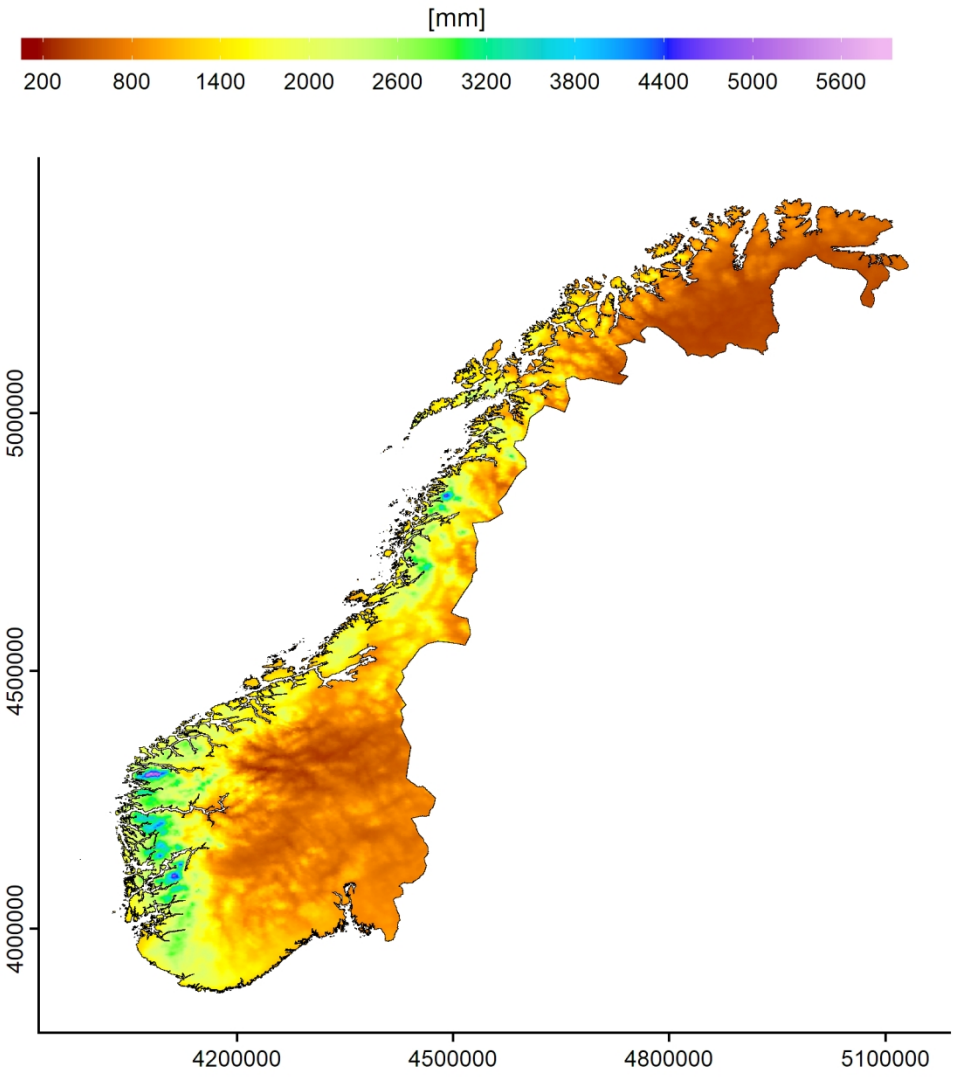

Annual HCLIM+RK precipitation climatology.

139x159mm (300 x 300 DPI)

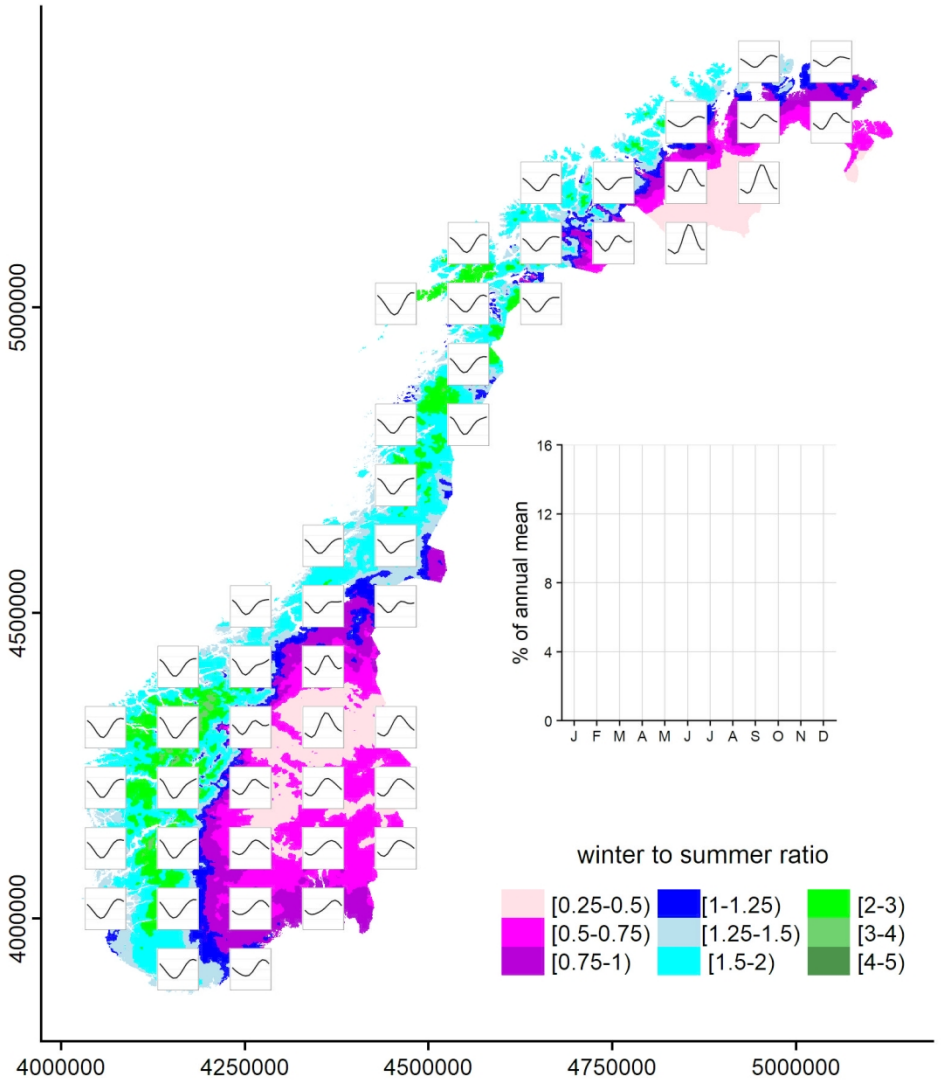

Distribution of winter (DJF) to summer (JJA) precipitation ratio over the domain and of the average yearly precipitation cycles over different 10000 km2 subdomains covering Norway. The inset box defines the range of axes that is the same for all the plots. The values are expressed as percentage to the total annual precipitation.

139x159mm (300 x 300 DPI)